The polarity protein Yurt associates with the lateral domain via basic and hydrophobic motifs embedded in its FERM domain

Charles Alende[1,2,#], Clémence L. Gamblin[1,2,#], François Corriveau[1,2], Alexandra Jetté[1,2], Frédérique Parent-Prévost[1,2], Cornélia Biehler[1,2,4,5], Nathalie Majeau[1,2], Mélanie Laurin[1,2,3], and Patrick Laprise[1,2,3,*]

[1]Centre de Recherche sur le Cancer, Université Laval, and [2]axe oncologie du Centre de Recherche du Centre Hospitalier Universitaire de Québec-UL, 9 McMahon, Québec, QC, G1R 3S3, Canada. [3]Département de biologie moléculaire, de biochimie médicale et de pathologie, Faculté de médecine, Université Laval. [4,5]Current affiliations: Faculty of Biological and Environmental Sciences, University of Helsinki, Helsinki 00790, Finland[4]; Institute of Biotechnology, University of Helsinki, Helsinki 00790, Finland[5].

[#]These authors contributed equally

[*]Author for correspondence: Patrick.Laprise@crchudequebec.ulaval.ca, Phone : (418) 525-4444 ext. 16959, Fax : (418) 691-5439

Key words: Yurt, membrane localization, FERM domain, FERM-adjacent domain, BH motif, epithelial morphogenesis, cell polarity.

Abstract

The subcellular distribution of the polarity protein Yrt is subjected to a spatio-temporal regulation in *D. melanogaster* embryonic epithelia. After cellularization, Yrt binds to the lateral membrane of ectodermal cells and maintains this localization throughout embryogenesis. During terminal differentiation of the epidermis, Yrt accumulates to septate junctions and is also recruited to the apical domain. While the mechanisms through which Yrt associates with septate junctions and the apical domain have been deciphered, how Yrt binds to the lateral membrane remains as an outstanding puzzle. Here, using an *in vivo* structure-function analysis, we show that the FERM domain of Yrt is necessary and sufficient for lateral localization. Our data also establish that the FERM domain of Yrt directly binds negatively charged phospholipids. Moreover, we demonstrate that positively charged amino acid motifs embedded within the FERM domain mediates Yrt membrane association. Finally, we provide evidence suggesting that Yrt association with the lateral membrane is functionally important. Overall, our study highlights the molecular basis of how Yrt associates with the lateral membrane before septate junction formation, a developmental time window where Yrt is required for segregation of lateral and apical domains. Our discoveries could thus contribute to further understanding of how epithelial cells acquire their polarized architecture.

Introduction

The plasma membrane of epithelial cells is segregated into an apical, a lateral, and a basal domain (Buckley and St Johnston, 2022; Tepass et al., 2001). This structural organization, which is referred to as epithelial cell polarity, supports many unidirectional functions of epithelia such as vectorial transport and secretion of selected molecules. Epithelial sheets display a selective permeability owing to occluding junctions sealing the intercellular space. In *D. melanogaster*, this function is fulfilled by septate junctions, which are established laterally (Banerjee et al., 2006).

The protein Yurt (Yrt) plays a crucial role in segregating apical and lateral domains in *D. melanogaster* embryonic epithelia at specific developmental stages (Laprise et al., 2006; Laprise et al., 2009). Yrt also controls septate junction permeability (Laprise et al., 2009). Yrt thus defines the functional architecture of epithelial cells, and impacts tissue morphogenesis and physiology (Hoover and Bryant, 2002; Laprise et al., 2009; Laprise et al., 2010). Yrt encloses a Four-point-one, Ezrin, Radixin, Moesin (FERM) domain at its N-terminus (Hoover and Bryant, 2002; Tepass, 2009). Yrt also contains a FERM-adjacent (FA) domain that is present in a subset of FERM family members (Baines, 2006; Tepass, 2009). The FERM and FA domain of Yrt both contribute to its oligomerization and function (Gamblin et al., 2014; Gamblin et al., 2018). The FA domain of Yrt is followed by a region lacking known protein domains designated as the variable region (VR), which ends with a putative PSD-95, DLG1, ZO-1 (PDZ) domain binding motif (PBM) (Laprise et al., 2006).

After cellularization, Yrt primarily localizes to the lateral membrane (Laprise et al., 2006). During terminal differentiation of epithelial tissues, Yrt accumulates at forming septate junctions and is

73 recruited apically (Laprise et al., 2006; Laprise et al., 2009). While the adhesion protein Neuroglian
74 (Nrg) recruits Yrt at septate junctions (Bieber et al., 1989; Laprise et al., 2009), the apical
75 localization of Yrt depends on a direct interaction of its FERM domain with the transmembrane
76 protein Crumbs (Crb) (Laprise et al., 2006). Binding of Yrt to Crb promotes cortical tension whilst
77 restricting apical membrane growth (Biehler et al., 2021; Osswald et al., 2022). We thus gained
78 insights into the molecular basis of Yrt association with septate junctions and the apical domain,
79 but it remains to be determined how Yrt associates with the lateral membrane basal to septate
80 junctions or prior to their formation. Furthermore, the functional importance of Yrt outside of
81 septate junctions or the apical Crb complex remains unexplored. In the present study, we performed
82 an *in vivo* structure-function analysis to define the molecular basis of Yrt association with the lateral
83 membrane in the embryonic ectoderm prior to septate junction genesis. We identified FERM
84 domain-embedded positively charged amino acid motifs contributing to Yrt membrane association
85 and pinpoint the functional importance of proper Yrt lateral localization.
86

87 ## Results and discussion

88 **The FERM domain targets Yrt laterally *in vivo***

89 The FERM domain protein Yrt primarily associates with the lateral domain prior to septate junction
90 formation in the embryonic ectoderm of stage 10 and 11 *D. melanogaster* embryos [(Laprise et al.,
91 2006); Fig. 1A, B]. Similarly, immunofluorescence performed with anti-FLAG antibodies showed
92 a lateral enrichment for FLAG-tagged full length (FL) Yrt at these developmental stages [(Gamblin
93 et al., 2014); Fig. 1A, C, L], whereas FLAG-green fluorescent protein (GFP) was distributed
94 throughout cells (Fig. 1D, L). This indicates that FLAG-Yrt represents a relevant model to perform
95 a structure-function analysis exploring the molecular basis of Yrt localization. We first investigated
96 the requirement for the FERM domain, the FA domain, and the VR (Hoover and Bryant, 2002;
97 Laprise et al., 2006; Tepass, 2009). We found that truncated Yrt proteins made of the FERM
98 domain alone or a combination of the FERM and FA domains showed a similar distribution to
99 FLAG-Yrt FL (Fig. 1A, E, F, L), whereas removal of the FERM domain totally abrogated
100 association of Yrt with the lateral membrane (Fig. 1A, G, L). In contrast, deletion of the FA domain
101 had no significant impact on Yrt lateral distribution (Fig. 1A, H, L). Moreover, truncations made
102 of the FA domain combined with the VR, the VR alone, or the VR amputated from the putative
103 PBM did not show clear enrichment at the lateral domain of cells (Fig. 1A, I-K, L). Together, these
104 data demonstrate that the FERM domain is necessary and sufficient for Yrt lateral targeting and
105 suggest that the FA domain and the VR have a limited, if any, role in promoting Yrt lateral
106 localization.

107

108 **Yrt binds to negatively charged phospholipids and putatively directly associates with the**
109 **plasma membrane**

110 The FERM domain of several proteins can directly associate with negatively charged phospholipids
111 such as phosphatidylinositol 4,5-bisphosphate [PI(4,5)P] via electrostatic interactions (Ehret et al.,
112 2023). To investigate whether the FERM domain of Yrt sustains such interactions, we decreased
113 the level of plasma membrane PI(4,5)P in S2 cells using ionomycin, which leads to PI(4,5)P
114 hydrolysis via phospholipase C activation. FLAG-Yrt was confined at the periphery in cells treated
115 with the vehicle DMSO, whereas it also localized in the cytoplasm in presence of ionomycin (Fig.
116 2A-C). In addition, purified Yrt FERM domain fused to GST showed affinity for
117 phosphatidylinositol phosphates immobilized on a membrane without discriminating between
118 PI(3)P, PI(4)P, PI(5)P, PI(3,4)P, PI(3,5)P, PI(4,5)P, or PI(3,4,5)P (Fig. 2D). The negatively
119 charged phosphate group(s) on these lipids is/are required for binding, as GST-FERM faintly
120 associated with Phosphatidylinositol (PI) (Fig. 2D). Of note, we cannot claim beyond any doubt
121 that GST-FERM binds to PI(3,4,5)P given that GST alone and GST-Grip, a PI(4,5)P specific probe,
122 also showed a weak association with this lipid (Fig. 2D). GST-FERM also associated with
123 Phosphatidic Acid (PA) and Phosphatidylserine (PS) (Fig. 2D). However, the FERM domain of
124 Yrt did not interact with Lysophosphatidic Acid (LPA), Lysophosphocholine (LPC),
125 Phosphatidylethanolamine (PE), Phosphatidylcholine (PC), or Sphingosine-1-phosphate (S1P)
126 (Fig. 2D). Together, these results show that the FERM domain of Yrt can directly associate with
127 several negatively charged phospholipids such as phosphatidylinositol phosphates but is not a
128 promiscuous lipid-binding protein. Yrt thus likely directly associates with the lateral membrane in
129 epithelial cells prior to septate junction assembly in *D. melanogaster* embryos, a developmental
130 time window where Yrt contributes to maintaining apical-basal polarity (Laprise et al., 2009).
131
132 **Positively charged amino acids within the FERM domain target Yrt to the lateral membrane**

133 Positively charged basic and hydrophobic (BH) amino acid motifs bind membrane phospholipids
134 via electrostatic interactions and contribute to membrane association of selected polarity proteins
135 (Bailey and Prehoda, 2015; Brzeska et al., 2010). Analysis of Yrt sequence revealed the presence
136 of two BH motifs within the FERM domain (regions of the black curve extending above the
137 threshold of 0.6 in Fig. 3A (Bailey and Prehoda, 2015)), which we referred to as BH1 and BH2.
138 Specifically, the BH1 and BH2 motifs span from amino acids 125-130 and 283-293, respectively.
139 *In silico* analysis showed that replacement of the positively charged lysine (K)124, arginine (R)132,
140 and K134 by negatively charged aspartate (D) residues abolished the BH properties of the BH1
141 motif (Fig. 3A, orange curve). Strikingly, FLAG-Yrt^{K124D,R132D,K134D} (FLAG-Yrt$^{BH1K/R>D}$ hereafter)
142 displayed a strongly decreased membrane to cytoplasmic ratio (Fig. 3B, D). Similarly, replacement
143 of K285 and K288 by D residues within the BH2 motif (FLAG-Yrt$^{BH2K>D}$) decreased Yrt
144 membrane enrichment, but the effect on Yrt localization resulting from BH2 mutations was less
145 pronounced than BH1 mutations (Fig. 3C, D). Of note, the BH2K>D mutant has a BH score close
146 to the threshold of 0.6 (Fig. 3A, purple curve). This potentially explains the weak impact of the
147 BH2K>D mutations on Yrt membrane localization. To test this hypothesis, we additionally
148 substituted the last two K residues of the BH2 motif by alanine (A) residues (K292 and K293;
149 FLAG-Yrt$^{BH2K>D,K>A}$). These mutations strongly decreased the BH score (Fig. 3A, blue curve) and
150 led to a significant reduction of Yrt membrane association in S2 cells, which was more important
151 than the delocalization of FLAG-Yrt$^{BH2K>D}$ and similar to FLAG-Yrt$^{BH1K/R>D}$ (Fig. 3E-J). Together,
152 these results demonstrate that BH1 and BH2 both contribute to target Yrt at the lateral membrane.
153

154 **Yrt lateral localization is functionally important**

155 Yrt overexpression is associated with a gain-of-function phenotype resulting from altered aPKC
156 and Crb functions (Biehler et al., 2021; Gamblin et al., 2014). Consequently, FLAG-Yrt expression

157 causes epithelial morphogenesis defects and a fully penetrant embryonic lethality phenotype
158 (Gamblin et al., 2014; Gamblin et al., 2018). Similarly, the membrane-associated protein FLAG-
159 FERM-FA is fully lethal. FLAG-Yrt$^{BH1K/R>D}$ and FLAG-Yrt$^{BH2K>D}$, which show cytoplasmic
160 delocalization with residual membrane association, showed a reduced ability to cause embryonic
161 lethality (Fig. 3B-D, 4A). Strikingly, the cytoplasmic truncations FLAG-Yrt$^{\Delta FERM}$, FA-VR, VR,
162 and VRΔPBM did not cause any lethality (Fig. 4A), although these constructs showed a similar
163 expression level to construct causing lethality (Fig. 4B). These results suggest that the gain-of-
164 function phenotype caused by Yrt overexpression reflects its lateral levels, indicating that Yrt plays
165 an important function at this subcellular location. Alternatively, our data may reflect the functional
166 importance of the FERM domain, as all truncations phenotypically silent or causing a weak
167 phenotype contain an impaired FERM domain. To distinguish between these two possibilities, we
168 used FLAG-Yrt^{5D}, which contains phosphomimetic mutations on aPKC target sites within the FA
169 domain while comprising an intact FERM domain (Gamblin et al., 2014). FLAG-Yrt^{5D} displayed
170 reduced membrane levels concomitant with cytoplasmic accumulation and is expressed at a similar
171 level to wild type FLAG-Yrt [Fig. 4B; (Gamblin et al., 2014)]. Importantly, expression of FLAG-
172 Yrt^{5D} had a modest impact on embryo survival with an 80% hatching rate (Fig. 4A). These results
173 are consistent with the idea that Yrt needs to associate with the lateral membrane to be fully
174 functional. These data also suggest that phosphorylation of Yrt by aPKC generates electrostatic
175 repulsion with negatively charged membrane phospholipids, as described for other aPKC
176 substrates (Bailey and Prehoda, 2015). This is in line with our previous observation that ectopic
177 localization of aPKC to the lateral domain displaces Yrt from the cortex (Biehler et al., 2021). Our
178 data thus further illuminate how Yrt function is antagonized by aPKC, witch represses Yrt
179 association with the lateral membrane and Yrt oligomerization (Gamblin et al., 2018).

180

181 Overall, our study shows that BH motifs within the FERM domain contribute to the localization of
182 Yrt at the lateral membrane putatively through direct association with negatively charged plasma
183 membrane phospholipids, including phosphatidylinositol phosphates. Mutations of the positively
184 charged residues contained in BH motifs decrease the Yrt gain of function phenotype, thereby
185 arguing that Yrt association with the lateral membrane is functionally important. Yrt could thus be
186 an important interactor of phosphatidylinositol phosphates allowing these molecules to perform
187 their known role in establishing and maintaining apical-basal polarity (Gassama-Diagne et al.,
188 2006; Krahn, 2020; Martin-Belmonte et al., 2007).

189

190 ## Materials and methods

191

192 **Molecular biology, transgenic fly lines, and *in vivo* expression of transgenes**

193 The In-Fusion cloning kit (Takara Bio) was used according to manufacturer's guideline to clone
194 cDNAs into pUASTattB (kindly provided by K. Basler, University of Zurich) and pGEX-6P-2 (GE
195 Healthcare Life Sciences). Full length (FL) *yrt* refers to the beta isoform, which includes all exons
196 of the *yrt* gene (Laprise et al., 2006). The resulting plasmids allowed for expression of the following
197 3xFLAG-tagged (N-terminus) Yrt proteins: ΔFERM (a.a. 1-56/346-972); VRΔPBM (a.a. 406-
198 969), BH1KR>D (K124D, R132D, K134D); BH2K>D (K285D, K288D); BH2K>D,K>A
199 (K285D, K288D, K292A, K293A). Genome Prolab (Sherbrooke, Canada) injected plasmids in *D.*
200 *melanogaster* embryos carrying an attP docking site (Groth et al., 2004). Specifically, transgenes
201 were inserted on the third chromosome (68E1; Bloomington *Drosophila* Stock Center (BDSC) line
202 24485, which was generated by the Basler's group) or the second chromosome (25C6; line
203 produced by Genome Prolab). The other constructs and fly lines used in this study were previously
204 described (Gamblin et al., 2014; Gamblin et al., 2018). We employed the UAS-GAL4 system to
205 express transgenes (Brand et al., 1994) using the da-GAL4 driver line (Wodarz et al., 1995).
206 Embryo staging was achieved according to the Atlas of *Drosophila* Development (Hartenstein,
207 1993).

208

209 **Cell culture and transfection**

210 S2 cells were grown at room temperature in Schneider's medium (Wisent Inc.) complemented with
211 10% fetal bovine serum (heat inactivated; Wisent Inc.), 50 units/ml penicillin, and 50 μg/ml
212 streptomycin (Life Technologies). When indicated, S2 cells were treated with 10 μM ionomycin

213 or the vehicle DMSO for 15 min. S2 cells were transfected at 60% confluency with FuGENE®
214 (Promega) with selected pUASTattB-based constructs together with pAct5c-GAL4.

215

216 **Immunofluorescence**

217 In preparation for immunofluorescence on *D. melanogaster* embryos, the chorion was removed by
218 a 5 min incubation in a solution of 3% sodium hypochlorite. Embryos were then washed with water,
219 fixed for 8 min in 11% formaldehyde (diluted in 60 mM PIPES, 30 mM EGTA, 1.2 mM $MgSO_4$)
220 under a heptane phase (1:1), and rinsed with PBS. Embryos were devitellinized by vigorous
221 agitation in methanol. Non-specific binding sites were blocked by a 1 h incubation in NGT (2%
222 normal goat serum, 0.3% Triton X-100 in PBS). S2 cells were fixed 24 h post-transfection with
223 4% paraformaldehyde (in PBS) for 15 min, permeabilized with PBS-0,1% Triton X-100, and
224 saturated for 1 h with a solution of 2% normal goat serum and 0.1% Triton X-100 in PBS.

225 The following primary antibodies were used overnight at 4°C: mouse anti-FLAG (M2, Sigma),
226 1/250 ; rabbit anti-Yrt (Biehler et al., 2020), 1:500. Following incubation with primary antibodies,
227 embryos and cells were washed three times for 20 min in PBS containing 0.3% or 0.1% Triton X-
228 100 (PBT), respectively, and incubated for 1 h at room temperature with Cy3- or Alexa Fluor 488-
229 conjugated secondary antibodies (1:400). Unbound secondary antibodies were washed-out with
230 PBT (3 times 20 min). Embryos and cells were mounted in Vectashield mounting medium (Vector
231 Labs) and imaged by confocal microscopy.

232

233 **Western blotting**

234 Dechorionated embryos were homogenized in lysis buffer (50 mM Tris-HCl pH 7.4, 150 mM
235 NaCl, 1 mM EDTA, 1% Triton X-100, 0.1 mM sodium orthovanadate, 0.1 mM
236 phenylmethylsulfonyl fluoride, 1 mM NaF, 10 µg/ml aprotinin, 10 µg/ml leupeptin and 0.7 µg/ml
237 pepstatin) at 4ºC and processed for SDS-PAGE and western blotting as described (Laprise et al.,
238 2002). The following primary antibodies were used: anti-FLAG M2 (Sigma-Adrich) 1:3000;
239 mouse anti-Actin (Novus Biologicals), 1:2000. Secondary antibodies were conjugated to HRP (GE
240 Healthcare) and diluted 1:2000.

241

242 **Protein purification and lipid binding assays**

243 GST and GST-FERM expression in BL21 (DE3) cells was induced by adding 0.1 mM IPTG to
244 bacterial cultures (O.D. of 0.6 at 600 nm) for 16 h at 16ºC. Proteins were then purified as previously
245 described (Maity et al., 2013). PIP Strips membranes (P-6001; Echelon Biosciences) were saturated
246 with 3% fatty acid free BSA (Sigma-Aldrich A8806) in PBS-Tween-20 0.1% for 1 h at room
247 temperature. Membranes were then incubated with 1 µg of GST, GST-FERM or PI(4,5)P2 Grip
248 (GST-PLC-d1-PH; Echelon Biosciences) following Echelon Biosciences' protocol. Protein-lipid
249 interactions were revealed by western blot using an anti-GST antibody (Santa Cruz
250 Biotechnology).

251

252 **Analysis of Yrt sequence**

253 Wild type and mutated sequences of the Yrt FERM domain were analyzed with the BH-search
254 algorithm [https://helixweb.nih.gov/bhsearch/ (Brzeska et al., 2010)].

255

256 **Quantification of membrane and cytoplasmic fluorescence intensity**

257 Quantification of fluorescence signal intensity was performed with FIJI (Schindelin et al., 2012).
258 In fly embryos, the polygon selection tool was used to generate a box, which was used to measure
259 both membrane and cytoplasmic intensity in each cell and the mean membrane/cytoplasm ratio
260 was determined. Ratios were determined in a total of 15 individual cells for each construct (5 non-
261 adjacent cells/embryo; 3 different embryos randomly selected from different experiments).

262

263 The freehand selection tool was used to individually select the whole membrane or cytoplasm in
264 S2 cells. This method was chosen, as the signal intensity was often irregular along the membrane
265 in S2 cells in contrast to what was observed *in vivo*. Total signal intensity (Raw Integrated Density;
266 RID) and the area of each box were recorded, and the membrane/cytoplasm ratios were calculated
267 as follow:

268 $$\text{Ratio} = \frac{(\text{membrane RID} \ / \ \text{membrane area})}{(\text{cytoplasm RID} \ / \ \text{cytoplasm area})}$$

269 Fluorescence ratio was quantified in 46 to 62 individual cells for each construct (15 to 23 cells per
270 experiment from 3-4 different experiments).

271

272 **Viability test**

273 One hundred newly laid embryos of each genotype were collected and placed on an apple plate at
274 25ºC for 72 h (this experiment was performed in triplicate). Larvae and dead embryos were then
275 scored, and the ratio of larvae on larvae plus dead embryos x 100 represents the hatching
276 percentage.

277

278 **Statistical analysis**

279 Statistical analyses were performed with Prism 8 (GraphPad Software). Membrane-to-cytoplasmic
280 ratio were presented as violin plots showing all individual measure as well as mean and quartiles.
281 Differences between individual groups were analyzed using Kruskal-Wallis test and post-hoc
282 Dunn's multiple comparison test, all compared to FLAG-Yrt FL. Adjusted p-values <0.05 were
283 considered statistically significant. In the case of ionomycin treatment in S2 cells, Mann-Whitney
284 test, two-tailed with α=0.05 was performed to assess differences between treatments. For viability
285 test, hatching data were presented as means ± SEM. Differences between individual groups were
286 analyzed by using Fisher's exact test (95% confidence intervals, two-tailed). P-values <0.05 were
287 considered statistically significant.

288

289 ## Figure legends

290 **Fig 1. The FERM domain of Yrt is necessary and sufficient for cortical targeting**

291 **(A)** Schematic representation of the FLAG-tagged full length and truncated proteins used in figure
292 1. **(B)** Stage 11 wild-type embryo stained for Yrt. The picture depicts a portion of the ventral
293 ectoderm, apical domain of cells is facing up. Scale bar represents 10 µm and also applies to C-K.
294 **(C-K)** FLAG immunostaining in stage 10-11 embryos expressing indicated FLAG-tagged
295 constructs. Panels show a portion of the ventral ectoderm oriented with the basal side of cells at
296 the bottom and the apical domain on top. **(L)** Violon plot showing the quantification of the
297 membrane to cytoplasmic ratio of each construct expressed in embryonic ectoderm. Kruskal-Wallis
298 test followed by Dunn's multiple comparison test compare different groups to FLAG-Yrt FL. Non-
299 significant (ns) > 0.05 ; **** $P \leq 0.0001$.

300

301 **Fig 2. The FERM domain of Yrt associates with negatively charged phospholipids**

302 (**A-B)** S2 cells were transfected with FLAG-Yrt and treated with the vehicle DMSO (A) or 10 µM
303 of ionomycin for 15 min (B). Cells were then processed for immunofluorescence and stained for
304 FLAG. Scale bar in A represents 5 µm and also applies to B. (**C**) Violon plot showing the
305 quantification of the membrane to cytoplasmic ratio in FLAG-Yrt expressing S2 cells treated with
306 DMSO or ionomycin. Mann-Whitney test, two-tailed with statistical significance set at $P < 0.05$,
307 compare the difference between cells treated with ionomycin or DMSO. **** $P \leq 0.0001$. (**D**) PIP
308 strip membranes were incubated with GST or indicated GST fusion proteins. Protein-lipid
309 interactions were revealed by western blotting using anti-GST antibodies.

310

311 **Fig 3. BH motifs embedded in the FERM domain contribute to Yrt lateral targeting**

312 (**A**) Analysis the Yrt FERM domain sequence for identification of BH motifs. The black line in
313 the upper panel shows the BH score (Y axis) along the wild-type sequence of the Yrt FERM domain
314 (X axis). Stretches of amino acids above the threshold of 0.6 (green horizontal dotted line) are
315 considered BH motifs (Bailey and Prehoda, 2015). The FERM domain of Yrt contains two BH
316 motifs, the sequence of which are shown in the lower panel (black font; the BH1 motif is underlined
317 and neighboring positively charged K and R residues are also shown). The lower panel also
318 displays mutations introduced in the BH1 (orange) and the BH2 (purple and blue) motifs. The BH
319 score of the mutant sequences is also shown in the upper panel according to the same color code.
320 (**B-C**) Immunostainings performed with anti-FLAG antibodies in stage 10-11 embryos expressing
321 indicated FLAG-tagged constructs. Panels show a portion of the ventral ectoderm oriented with
322 the apical domain on top. Scale bar in B represents 10 μm and also applies to C. (**D**) Violon plot
323 showing the quantification of the membrane to cytoplasmic ratio for FLAG-Yrt FL, FLAG-
324 Yrt$^{BH1K/R>D}$ and FLAG-Yrt$^{BH2K>D}$ expressed the embryonic ectoderm. (**E-G**) Immunostainings
325 performed with anti-FLAG antibodies in S2 cells expressing indicated FLAG-tagged constructs.
326 Scale bar in **E** represents 5 μm and also applies to F-G. (**J**) Violon plot showing the quantification
327 of the membrane to cytoplasmic ratio for FLAG-GFP, FLAG-Yrt FL, FLAG-Yrt$^{BH1K/R>D}$, FLAG-
328 Yrt$^{BH2K>D}$ and FLAG-Yrt $^{BH2K>D,K>A}$ expressed in S2 cells. (**D, J**) Kruskal-Wallis test followed by
329 Dunn's multiple comparison test compare different groups to FLAG-Yrt FL. * $P = 0.0200$; ** $P =$
330 0.0042; **** $P \leq 0.0001$.

331

332 **Fig 4. Yrt association with the lateral membrane is functionally important**

333 (**A**) Histogram showing the hatching rate, calculated in percentage, of embryos expressing
334 indicated FLAG-tagged Yrt proteins. Error bars represent SEM, and statistical significance was
335 assessed by using Fisher's exact test (FL: $n = 269$; FERM-FA: $n = 234$; ΔFERM: $n = 270$; FA-VR:
336 $n = 233$; VR: $n = 269$; VRΔPBM: $n = 235$; BH1K/R>D: $n = 237$; BH2K>D: $n = 265$; 5D: $n = 247$).
337 (**B**) Western blot showing the relative expression of indicated FLAG-tagged constructs in stage 11-
338 12 embryos. Actin was used as loading control.

Acknowledgments

The authors would like to acknowledge K. Basler and the Bloomington *Drosophila* Stock Center for reagents. Flybase was used as an important database for this work. This work was supported by operating grants from the Canadian Institute of Health Research (CIHR) to P.L. (PJT-185951) and M.L. (PJT-178198). F.C. is supported by a scholarship from FRQ-S, and C. B. is a postdoctoral Europe Horizon MSCA-PF grantee.

Author contributions

P.L. conceived the project. C.A., C.G., F.C., F.P.P. and N.M. performed experiments and/or prepared reagents and contributed to data analysis. C.B. trained C.A. and contributed to initial *in vivo* analyses. A.J. performed statistical analysis and assembled figures with C.G. and C.A. P.L. wrote the manuscript, which was proofread by co-authors. P.L. and M.L. secured funding.

Competing interests

The authors declare no competing financial interests.

354 **REFERENCES**

355 Bailey, M.J., and K.E. Prehoda. 2015. Establishment of Par-Polarized Cortical Domains via
356 Phosphoregulated Membrane Motifs. *Developmental cell*. 35:199-210.

357 Baines, A.J. 2006. A FERM-adjacent (FA) region defines a subset of the 4.1 superfamily and is a
358 potential regulator of FERM domain function. *BMC Genomics*. 7:85.

359 Banerjee, S., A.D. Sousa, and M.A. Bhat. 2006. Organization and function of septate junctions:
360 an evolutionary perspective. *Cell Biochem Biophys*. 46:65-77.

361 Bieber, A.J., P.M. Snow, M. Hortsch, N.H. Patel, J.R. Jacobs, Z.R. Traquina, J. Schilling, and
362 C.S. Goodman. 1989. Drosophila neuroglian: a member of the immunoglobulin
363 superfamily with extensive homology to the vertebrate neural adhesion molecule L1. *Cell*.
364 59:447-460.

365 Biehler, C., K.E. Rothenberg, A. Jette, H.M. Gaude, R. Fernandez-Gonzalez, and P. Laprise.
366 2021. Pak1 and PP2A antagonize aPKC function to support cortical tension induced by
367 the Crumbs-Yurt complex. *Elife*. 10.

368 Biehler, C., L.T. Wang, M. Sevigny, A. Jette, C.L. Gamblin, R. Catterall, E. Houssin, L.
369 McCaffrey, and P. Laprise. 2020. Girdin is a component of the lateral polarity protein
370 network restricting cell dissemination. *PLoS Genet*. 16:e1008674.

371 Brand, A.H., A.S. Manoukian, and N. Perrimon. 1994. Ectopic expression in Drosophila.
372 *Methods Cell Biol*. 44:635-654.

373 Brzeska, H., J. Guag, K. Remmert, S. Chacko, and E.D. Korn. 2010. An experimentally based
374 computer search identifies unstructured membrane-binding sites in proteins: application to
375 class I myosins, PAKS, and CARMIL. *The Journal of biological chemistry*. 285:5738-
376 5747.

377 Buckley, C.E., and D. St Johnston. 2022. Apical-basal polarity and the control of epithelial form
378 and function. *Nature reviews. Molecular cell biology*.

379 Ehret, T., T. Heissenberg, S. de Buhr, C. Aponte-Santamaria, C. Steinem, and F. Grater. 2023.
380 FERM domains recruit ample PI(4,5)P(2)s to form extensive protein-membrane
381 attachments. *Biophys J*. 122:1325-1333.

382 Gamblin, C.L., E.J. Hardy, F.J. Chartier, N. Bisson, and P. Laprise. 2014. A bidirectional
383 antagonism between aPKC and Yurt regulates epithelial cell polarity. *The Journal of cell*
384 *biology*. 204:487-495.

385 Gamblin, C.L., F. Parent-Prevost, K. Jacquet, C. Biehler, A. Jette, and P. Laprise. 2018.
386 Oligomerization of the FERM-FA protein Yurt controls epithelial cell polarity. *The*
387 *Journal of cell biology*.

388 Gassama-Diagne, A., W. Yu, M. ter Beest, F. Martin-Belmonte, A. Kierbel, J. Engel, and K.
389 Mostov. 2006. Phosphatidylinositol-3,4,5-trisphosphate regulates the formation of the
390 basolateral plasma membrane in epithelial cells. *Nature cell biology*. 8:963-970.

391 Groth, A.C., M. Fish, R. Nusse, and M.P. Calos. 2004. Construction of transgenic Drosophila by
392 using the site-specific integrase from phage phiC31. *Genetics*. 166:1775-1782.

393 Hartenstein, V. 1993. Atlas of Drosophila development. Cold Spring Harbor Laboratory Press,
394 Plainview, N.Y. v, 57 p. pp.

395 Hoover, K.B., and P.J. Bryant. 2002. Drosophila Yurt is a new protein-4.1-like protein required
396 for epithelial morphogenesis. *Dev Genes Evol*. 212:230-238.

397 Krahn, M.P. 2020. Phospholipids of the Plasma Membrane - Regulators or Consequence of Cell
398 Polarity? *Front Cell Dev Biol*. 8:277.

399 Laprise, P., S. Beronja, N.F. Silva-Gagliardi, M. Pellikka, A.M. Jensen, C.J. McGlade, and U.
400 Tepass. 2006. The FERM protein Yurt is a negative regulatory component of the Crumbs
401 complex that controls epithelial polarity and apical membrane size. *Developmental cell*.
402 11:363-374.

403 Laprise, P., P. Chailler, M. Houde, J.F. Beaulieu, M.J. Boucher, and N. Rivard. 2002.
404 Phosphatidylinositol 3-kinase controls human intestinal epithelial cell differentiation by
405 promoting adherens junction assembly and p38 MAPK activation. *The Journal of*
406 *biological chemistry*. 277:8226-8234.

407 Laprise, P., K.M. Lau, K.P. Harris, N.F. Silva-Gagliardi, S.M. Paul, S. Beronja, G.J. Beitel, C.J.
408 McGlade, and U. Tepass. 2009. Yurt, Coracle, Neurexin IV and the Na(+),K(+)-ATPase
409 form a novel group of epithelial polarity proteins. *Nature*. 459:1141-1145.

410 Laprise, P., S.M. Paul, J. Boulanger, R.M. Robbins, G.J. Beitel, and U. Tepass. 2010. Epithelial
411 polarity proteins regulate Drosophila tracheal tube size in parallel to the luminal matrix
412 pathway. *Current biology : CB*. 20:55-61.

413 Maity, R., J. Pauty, J. Krietsch, R. Buisson, M.M. Genois, and J.Y. Masson. 2013. GST-His
414 purification: a two-step affinity purification protocol yielding full-length purified proteins.
415 *J Vis Exp*:e50320.

416 Martin-Belmonte, F., A. Gassama, A. Datta, W. Yu, U. Rescher, V. Gerke, and K. Mostov. 2007.
417 PTEN-mediated apical segregation of phosphoinositides controls epithelial
418 morphogenesis through Cdc42. *Cell*. 128:383-397.

419 Osswald, M., A. Barros-Carvalho, A.M. Carmo, N. Loyer, P.C. Gracio, C.E. Sunkel, C.C.F.
420 Homem, J. Januschke, and E. Morais-de-Sa. 2022. aPKC regulates apical constriction to
421 prevent tissue rupture in the Drosophila follicular epithelium. *Current biology : CB*.

422 Tepass, U. 2009. FERM proteins in animal morphogenesis. *Curr Opin Genet Dev*. 19:357-367.

423 Tepass, U., G. Tanentzapf, R. Ward, and R. Fehon. 2001. Epithelial cell polarity and cell
424 junctions in Drosophila. *Annu Rev Genet*. 35:747-784.

425 Wodarz, A., U. Hinz, M. Engelbert, and E. Knust. 1995. Expression of crumbs confers apical
426 character on plasma membrane domains of ectodermal epithelia of Drosophila. *Cell*.
427 82:67-76.

428

429

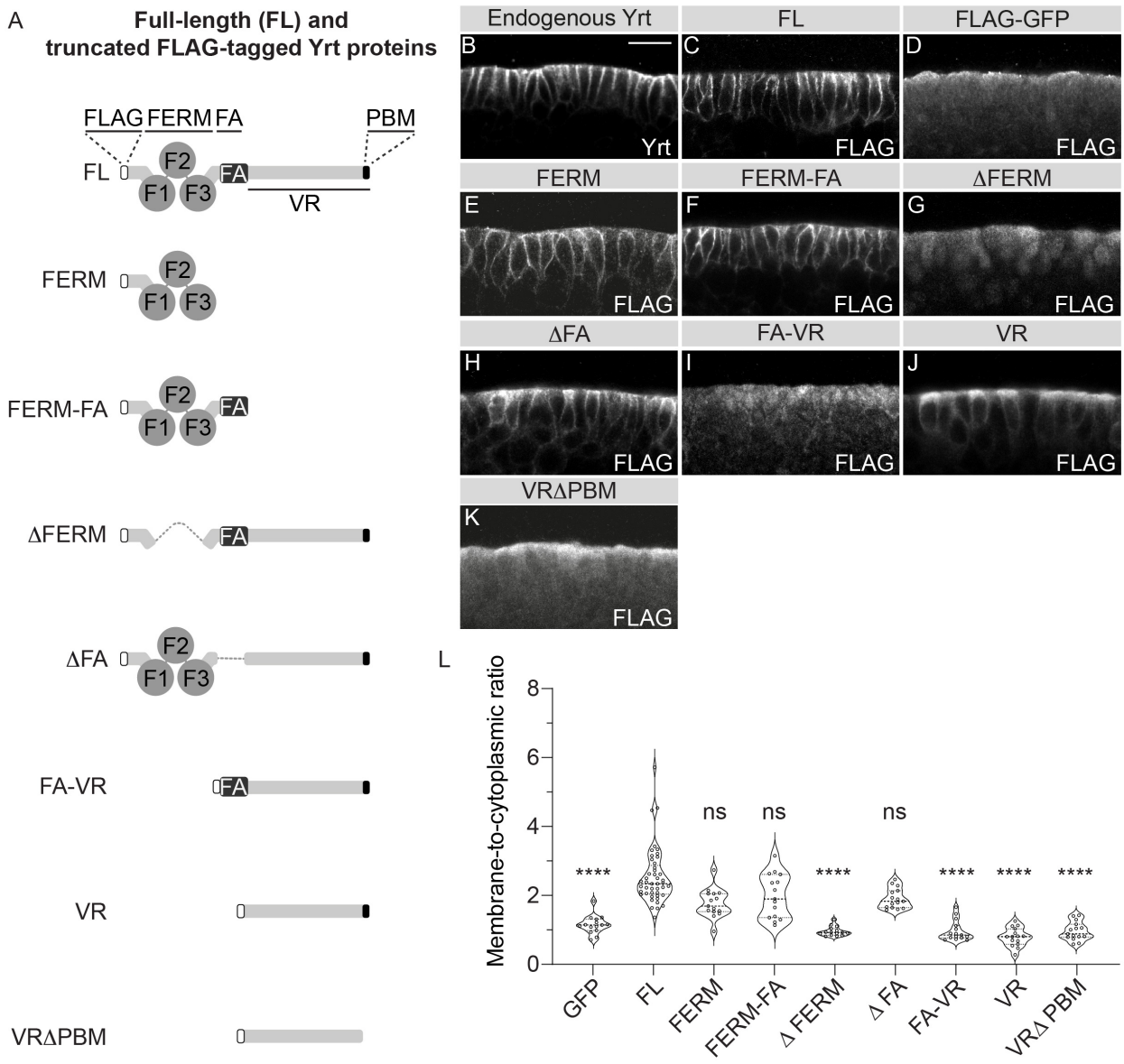

Alende et al. Fig. 1

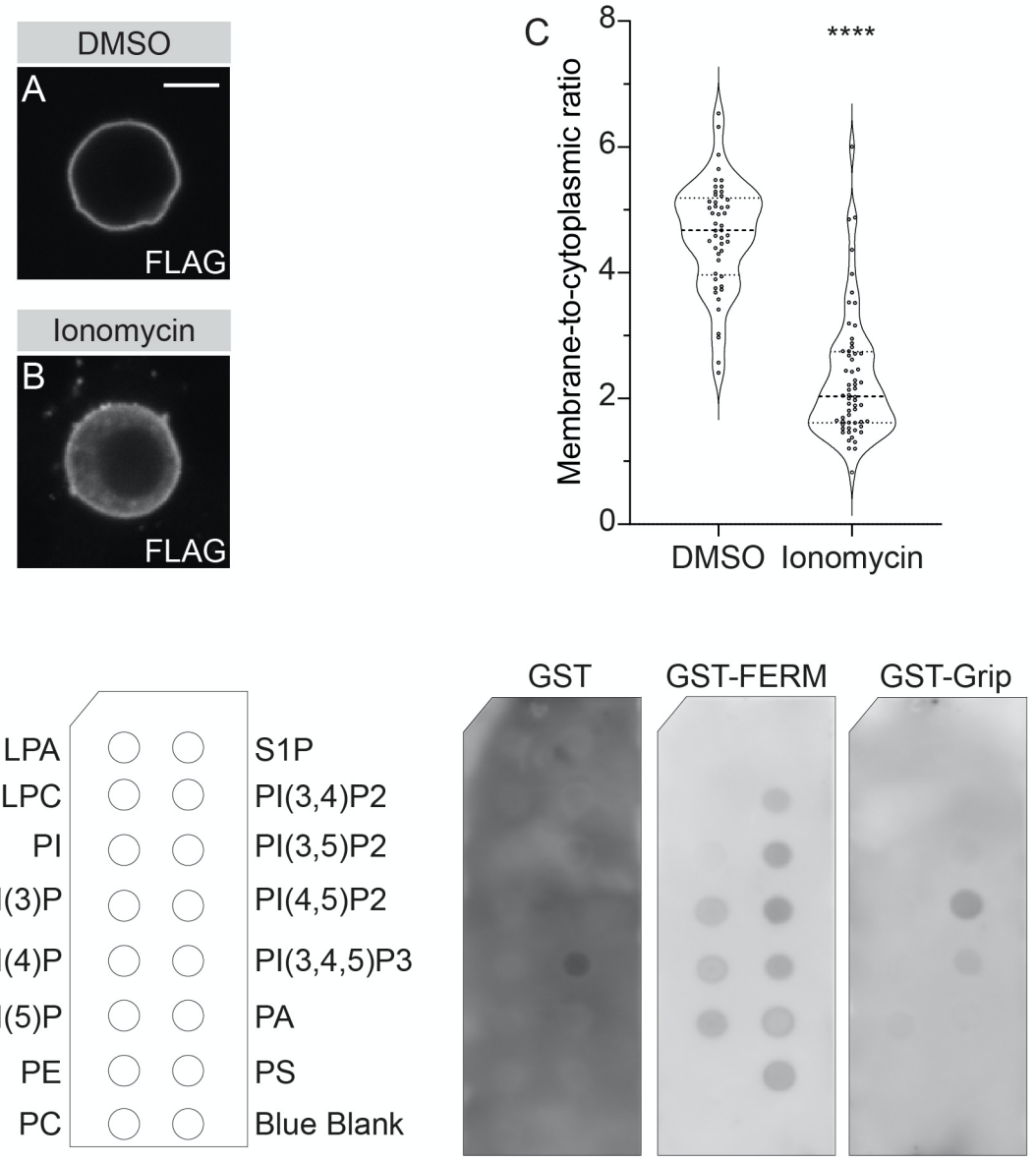

Alende et al. Fig. 2

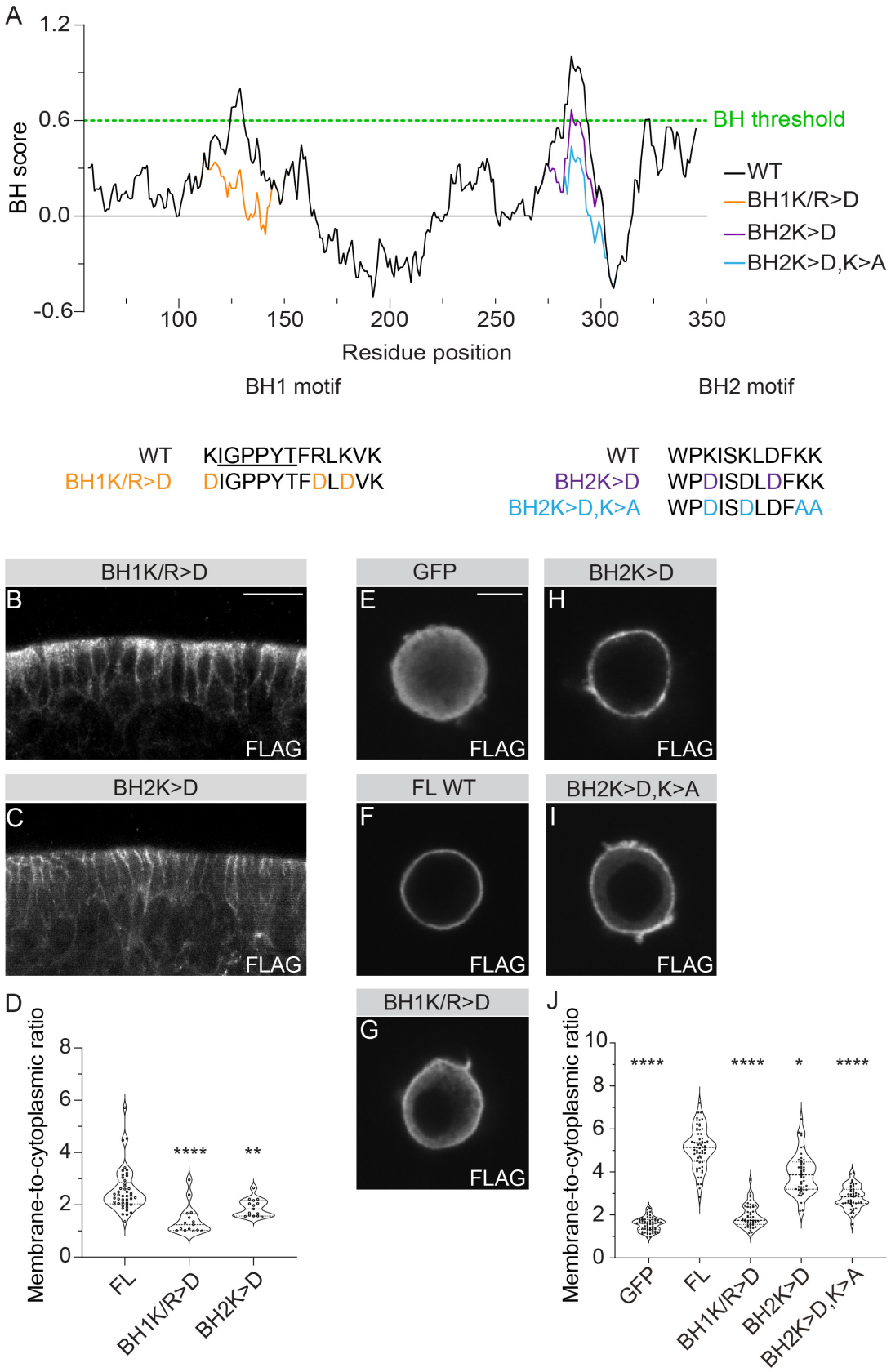

Alende et al. Fig. 3

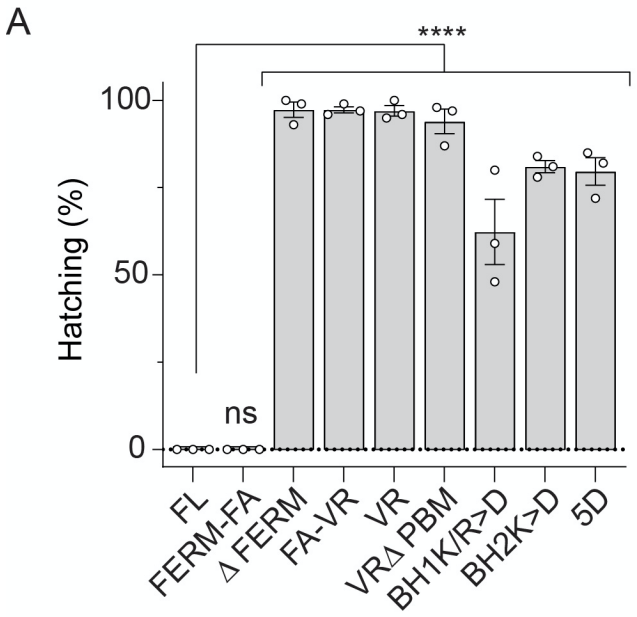

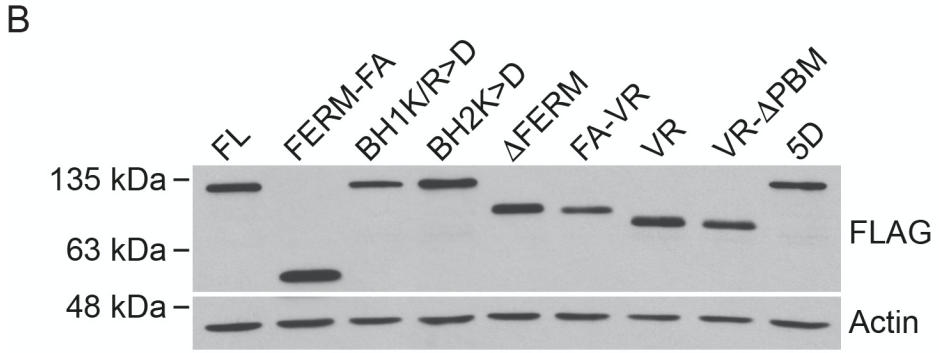

Alende et al. Fig. 4